Iranian Journal of Medical Physics

ijmp.mums.ac.ir

Continuous Visual Stimulation Is Associated With Reduced Occipital Brain Temperature Measured By Magnetic Resonance Spectroscopy Thermometry

Abdul Nashirudeen Mumuni[1*], Mohammed Nasir Abubakari[1]

1. Department of Medical Imaging, School of Allied Health Sciences, University for Development Studies, Tamale, Ghana.

ARTICLE INFO

Article type:
Original Paper

Article history:
Received: Apr 06, 2024
Accepted: July 07, 2024

Keywords:
Brain
Magnetic Resonance Spectroscopy
Thermometry
Visual Cortex
Visual Stimulation

ABSTRACT

Introduction: There is paucity of information about the impact of different neuroactivation paradigms on brain temperature changes in functional magnetic resonance spectroscopy (fMRS) studies. Magnetic resonance spectroscopy (MRS) thermometry was used to estimate the pattern of brain temperature changes with single and continuous neuroactivation paradigms.

Material and Methods: Single-voxel MRS data was acquired from the visual cortex of four healthy volunteers using the standard spin-echo Point-RESolved Spectroscopy (PRESS) localization sequence synchronized to single and continuous visual stimulation paradigms at 3.0 tesla (T). Blood oxygenation level-dependent (BOLD) effects were estimated from changes in spectral peak height, linewidth, and area. Brain temperature was calculated by substituting the frequency offset of the water peak relative to the N-acetyl aspartate (NAA), creatine (Cr), and choline (Cho) peaks into previously deduced calibration equations for each reference peak. BOLD and temperature changes from baseline were compared by paired t-test at a significance level of $p < 0.05$.

Results: In the single activation paradigm, Cho ($p = 0.01$) peak height, and NAA ($p = 0.01$) and Cr ($p = 0.02$) peak areas showed significant changes without significant brain temperature changes relative to all three peaks ($p > 0.05$). In the continuous activation paradigm, Cr ($p = 0.04$) peak width showed significant change, with significant brain temperature changes relative to all three reference peaks ($p < 0.05$).

Conclusion: Brain temperature significantly reduced with continuous visual activation but not with single visual activation paradigms.

►*Please cite this article as:*
Mumuni AN, Abubakari MN. Continuous Visual Stimulation Is Associated With Reduced Occipital Brain Temperature Measured By Magnetic Resonance Spectroscopy Thermometry. Iran J Med Phys 2024; 21: 402-408. 10.22038/ijmp.2024.79155.2399.

Introduction

Metabolic activities associated with normal brain function result in physiological brain temperature fluctuations within 2-4 ^{o}C [1]. While functional magnetic resonance spectroscopy (fMRS) is tailored for probing both brain metabolism and function, it does not directly offer information about the associated temperature variations. Functional MRS exploits the blood oxygenation level-dependent (BOLD) contrast mechanism during neuroactivation to offer information about spectral responses to a stimulus [2,3].

The BOLD effect arises when neurons respond to an external stimulus, which raises their physiological activity above baseline, causing more oxygenated blood to flow to the activated neurons. The presence of oxygenated blood in such neurons creates susceptibility gradients associated with T2* contrast to spread within blood-carrying vessels and tissue near those vessels [4]. The T2* contrast in MRS can be recorded by a localized spin-echo MRS pulse sequence [5]. The recorded free induction decay (FID) signal is characterized by the FID amplitude of the first sampling point at the center of the echo (A_{FID}), the FID decay rate (1/T2*), and the integral of the FID (I_{FID}) [6]. After Fourier transformation of the FID, I_{FID}, A_{FID}, and T2* correlate with spectral peak height (H_S), linewidth at half peak height ($\Delta\upsilon_{1/2}$), and spectral peak area (A_S) [2]. Spectral response to the BOLD effect manifests as increased H_S and A_S and decreased $\Delta\upsilon_{1/2}$ [5-7].

It has been established that ambient temperature and motor activity, such as exercise, increase brain metabolism, which is thought to be linked to a moderate increase in brain temperature [8-11]. Findings from brain activation studies with respect to temperature variations are, however, inconsistent. This is particularly due to the duration, intensity, and depth of brain tissue being activated. These factors ultimately influence the balance between metabolic heat production, heat removal by blood flow, and heat conductance, which together modulate brain temperature [12]. Meanwhile, brain temperature monitoring during fMRS studies is necessary because such experiments could potentially cause a significant

*Corresponding Author: Tel: +233 206 212 210; Email: mnashiru@uds.edu.gh

increase in brain temperature and other undesirable physiological effects such as headaches. The technique of measuring brain temperature, in this case, is known as MRS thermometry. The technique is based on the measurement of the shift in the resonance frequency of the water peak (ΔH_2O) away from the spectral peak of N-acetyl aspartate (NAA) in most cases [13-16]; indeed, other studies have measured this displacement of the water peak relative to the creatine (Cr) and choline (Cho) spectral peaks as well [17-19]. The frequency difference is then converted to a temperature value using an appropriate mathematical equation [17]. MRS thermometry can be implemented in both single-voxel [13,14,17] and spectroscopic imaging [15,16] techniques of MRS.

Measured brain temperature is a relevant physiological parameter that can serve as an indication for many health conditions such as brain injury, stroke, trauma, headache, epilepsy, neurodegenerative, and mood disorders. Even though centrally-mediated mechanisms often explain brain temperature changes, little is reported about the spatial and temporal distributions of brain temperature fluctuations [20]. The temporal resolution for fMRS data acquisition has been investigated previously [2,3]. Therefore, it can be inferred that the recorded BOLD signal acquired at a given temporal resolution inherently contains the temperature information in the spectra in the frequency domain. What needs to be clarified is, therefore, the respective temperature effects that arise from different stimulation paradigms used in fMRS experiments.

The aim of this study was, therefore, to quantitatively assess the pattern of brain temperature change in response to single and continuous visual activation paradigms for functional MRS acquisitions. In addition, the feasibility of implementing MRS thermometry in a conventional clinical dynamic MR spectroscopy acquisition was explored. MR spectroscopy is sensitive to motion artifacts, making motor neuroactivation paradigms undesirable for fMRS acquisitions; visual stimulation of the visual cortex region of the brain of stable human subjects, as implemented in this study, is thus the most preferred paradigm [2,3,6].

Materials and Methods

Subjects

Four healthy volunteers (3 males/1 female, mean age ±SD=32.3±3.0 years) gave informed consent to participate in the study, which the West of Scotland Research Ethics Committee 4 (WoSREC4) approved. All volunteers were screened for neurological disorders and contraindications with magnetic resonance imaging (MRI).

Visual stimulus

Visual activation of the occipital brain region was carried out by presenting to each volunteer, through a bifocal lens ensemble, an in-house 8 Hz black/white pattern-reversal checkerboard played from a laptop computer.

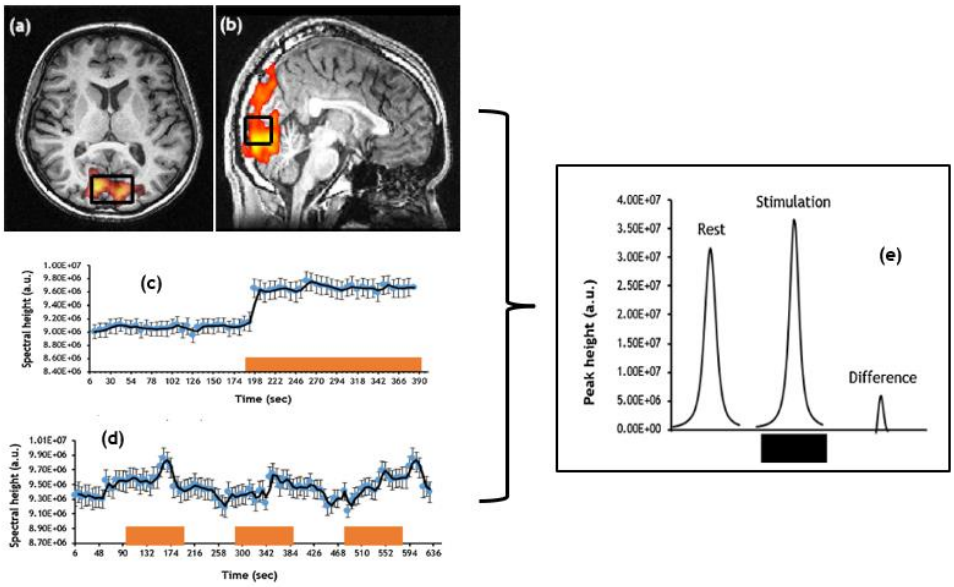

Figure 1. Axial (a) and sagittal (b) views of the localized volume within the activated visual cortex region; time course of the BOLD effect on spectral height ($\%\Delta H_S$) during the single (c) and continuous (d) stimulation paradigms. Estimation of the BOLD effect on spectral peak height (e).

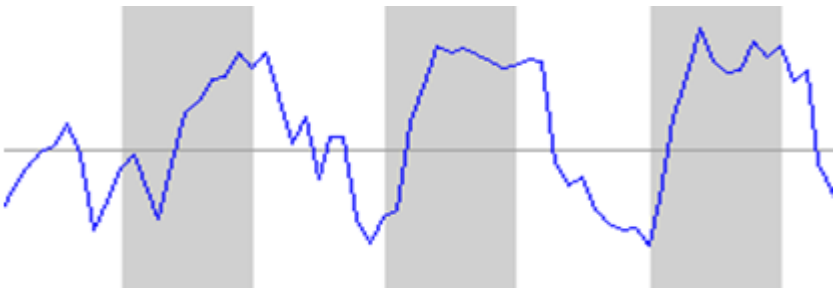

Figure 2. Hemodynamic occipital brain response plot associated with visual activation in the fMRI experiment; the grey bars indicate the stimulus periods; the white bars indicate the rest periods

Functional MR spectroscopy

Experiments were conducted on a 3.0 T General Electric magnet using an 8-channel radiofrequency receive brain imaging coil. Before the fMRS acquisitions, functional MRI scans were conducted on each volunteer to locate the precise site of activation and its size for placement of the fMRS single-voxel (Figure 1a-b). An activation paradigm comprising three 30-second rest and three 30-second stimulation periods was used (Figure 2), as previously described [2]. Beyond using the visualized onscreen activation map on the MR images to plan the fMRS voxel placement, the fMRI data was not further analyzed.

Two visual stimulation paradigms were designed for the fMRS experiments: "single" (Figure 1c) and "continuous" (Figure 1d) visual stimulation paradigms, as previously described [2]. In the single visual stimulation paradigm, a 192-second rest (black screen display) period was followed by a 192-second stimulation (8-Hz flashing black/white reversal display) period, consisting of a total duration of 384 seconds (in the order OFF-ON). In the continuous visual stimulation paradigm, three rest periods were interleaved with three stimulation periods, each of equal duration of 96 seconds; the total duration of the continuous stimulation paradigm was, therefore, 576 seconds (in the order OFF-ON-OFF-ON-OFF-ON).

The fMRS data was recorded by employing the clinical Point-RESolved Spectroscopy (PRESS) localization scheme [2]. A voxel of dimensions 20 S/I x 20 A/P x 30 R/L mm^3 was planned on the fMRI-defined activated occipital brain region (Figure 1a-b). Signals from tissue outside the voxel and tissue water were annulled using outer-volume and CHEmical Shift Selective suppression modules, respectively. Signal localization was achieved using *TE/TR* = 23/3000 ms, bandwidth = 5000 Hz, and NEX = 2; the signal averages (NSA) value was ~~between~~ 64 and 32 for the single and continuous activations, respectively.

Spectral analysis

The acquired spectra were processed on two spectral analysis platforms to obtain results for the BOLD and temperature changes. Analysis for the BOLD effects was performed on the SAGE platform (version 7; GE Healthcare, Little Chalfont, Buckinghamshire, UK); the temperature effects were analyzed using the jMRUI software package (version 6.0; URL http://www.mrui.uab.es/mrui/).

To quantify the BOLD effects, the raw FIDs were corrected for eddy-current effects, summed up, and converted to frequency-domain MR spectra, corrected for phase and baseline distortions. This process reduced the effects of noise and susceptibility artifacts in the data. The peaks to be quantified were then manually selected to automatically estimate rough values of the amplitude, linewidth, and frequency of the peaks, as well as the standard deviation of noise in the spectrum. A nonlinear least squares minimization technique based on the Levenberg-Marquardt (LM) model was implemented using rough estimates to calculate the height, linewidth, and area of the spectral peaks of interest. The LM scheme was implemented to both locally calculate these three parameters for each line of data (Figure 1c-d) and to quantify the percentage of BOLD changes in response to the stimulus (Figure 1e).

To quantify the temperature effects, the raw data was filtered using a Lorentzian filter for line broadening, Fourier transformed, and automatically baseline and phase-corrected. All processed spectra were judged to be of good quality if their linewidths did not exceed 10 Hz, their baseline was fairly regular, and the major peaks (i.e., NAA, Cr, and Cho) did not shift by more than 0.2 ppm from their expected resonant frequencies.

MRS thermometry

The spectral peaks of N-acetyl aspartate (NAA), creatine (Cr), and choline (Cho) were checked to confirm that they were at their respective positions on the resonance frequency axis. The water peak was selected in the jMRUI software (Figure 3) to check and record the drift in its frequency position.

The frequency drift of the water peak (ΔH_2O) from each metabolite peak position (Δ_{met}) was estimated as ($\Delta H_2O - \Delta_{met}$). The resonance frequency values for the metabolites (Δ_{met}) were NAA = 2.01 ppm, Cr = 3.03 ppm, and Cho = 3.20 ppm.

The following previously determined regression equations were used to convert each referenced frequency shift ($\Delta H_2O - \Delta_{met}$) to brain temperature ($T_{brain}$) [17]:

$$\text{NAA; } T_{brain} = 1.3280(\Delta H_2O - 2.01) + 32.626 \quad (1)$$

$$\text{Cr; } T_{brain} = 1.3275(\Delta H_2O - 3.03) + 33.987 \quad (2)$$

Cho; $T_{brain} = 1.3275(\Delta H_2O - 3.20) + 34.213$ (3)

Each equation was used to determine brain temperature for the rest and stimulation acquisitions, in order to estimate temperature changes from baseline following neuroactivation.

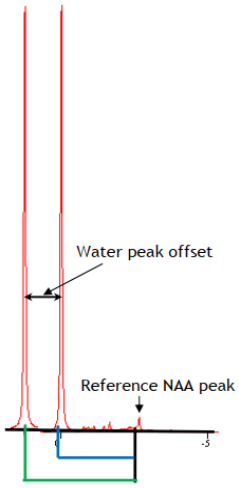

Figure 3. Temperature-dependent water frequency shift from its normal position, away from the reference NAA metabolite spectral peak

Estimation of BOLD and temperature changes

The BOLD and temperature changes were both calculated from the following:

$\%\Delta X = [(X_{Stimulation} - X_{Rest})/X_{Rest}] \times 100\%$ (4)

where $X_{Stimulation}$ and X_{Rest} are the spectral peak parameters associated with the stimulation and rest periods, respectively.

Negative percentage changes were recorded for reductions, and positive percentage changes were recorded for increases in the respective parameters for BOLD and temperature.

Statistical analysis

The significance of the differences in BOLD and temperature changes between the baseline and activation periods was assessed using a paired t-test, assuming data normality. The linearity of the relationship between BOLD and temperature changes was assessed by the Pearson correlation test. All statistical tests were significant at $p < 0.05$. All statistical tests were performed using Minitab (version 17).

Results

Sample hemodynamic occipital brain response plots of the spectral heights are shown for the rest and stimulation periods in Figures 4a-b.

In the single activation paradigm (Table 1), only the percentage changes in the areas of the NAA ($p = 0.01$) and Cr ($p = 0.02$) peaks were significant, while the change in the height of the Cho peak was significant ($p = 0.01$). Temperature change was not statistically significant relative to all three reference peaks ($p > 0.05$).

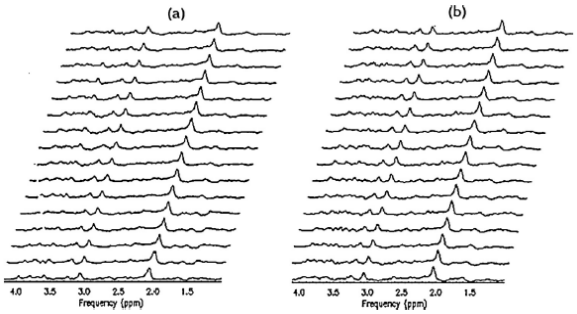

Figure 4. Hemodynamic occipital brain response plots for the rest (a) and stimulus (b) periods in the continuous neuroactivation paradigm in the fMRS experiment

In the continuous activation paradigm (Table 2), only the percentage change in the width of the Cr peak was significant ($p = 0.04$). However, percentage changes in temperature were statistically significant relative to all three reference peaks ($p < 0.05$).

Generally, visual cortex temperature reduced with neural activation (Tables 1-2; Figures 5-6), and the reduction was statistically significant with the continuous (Figure 6) but not with the single activation paradigm (Figure 5). However, the only female volunteer in the study showed rather increased visual cortex temperature with the single activation paradigm.

Only the percentage change in NAA peak height had a significant positive correlation with visual cortex temperature variation in the single activation paradigm ($r = 0.998$, $p = 0.002$).

Table 1. Percentage BOLD and temperature changes in the single activation paradigm

Peak	$\Delta H_S\% \pm$ SE (p-value)	$\Delta \upsilon_{1/2}\% \pm$ SE (p-value)	$\Delta A_S\% \pm$ SE (p-value)	$\Delta T\% \pm$ SE (p-value)
NAA	0.49 ± 0.18 (0.72)	-5.59 ± 1.94 (0.07)	11.17 ± 1.94 (0.01)	-2.05 ± 1.69 (0.32)
Cr	0.78 ± 0.24 (0.53)	-0.85 ± 0.28 (0.79)	7.35 ± 0.94 (0.02)	-2.56 ± 1.22 (0.13)
Cho	2.24 ± 0.47 (0.01)	-2.10 ± 0.95 (0.73)	7.59 ± 0.84 (0.11)	-3.66 ± 1.80 (0.14)

Table 2. Percentage BOLD and temperature changes in the continuous activation paradigm

Peak	$\Delta H_S\% \pm$ SE (p-value)	$\Delta \upsilon_{1/2}\% \pm$ SE (p-value)	$\Delta A_S\% \pm$ SE (p-value)	$\Delta T\% \pm$ SE (p-value)
NAA	1.09 ± 0.41 (0.14)	-1.09 ± 0.35 (0.45)	0.85 ± 0.47 (0.68)	-2.94 ± 0.70 (0.02)
Cr	0.18 ± 0.09 (0.90)	-3.05 ± 0.97 (0.04)	0.86 ± 0.35 (0.71)	-4.21 ± 0.71 (0.01)
Cho	1.41 ± 0.65 (0.25)	-2.62 ± 0.93 (0.12)	2.09 ± 0.63 (0.54)	-2.75 ± 0.44 (0.01)

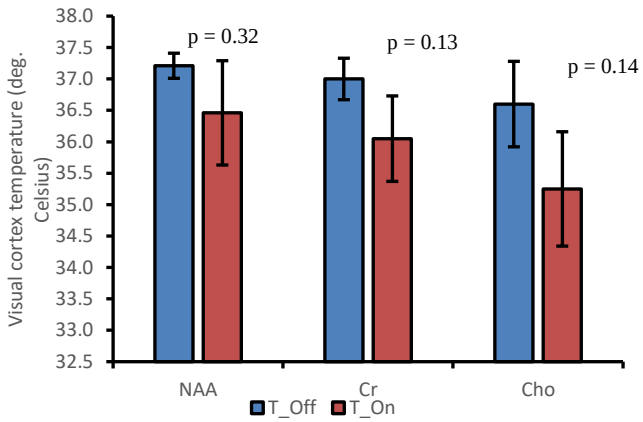

Figure 5. Visual cortex temperature change with the single activation paradigm

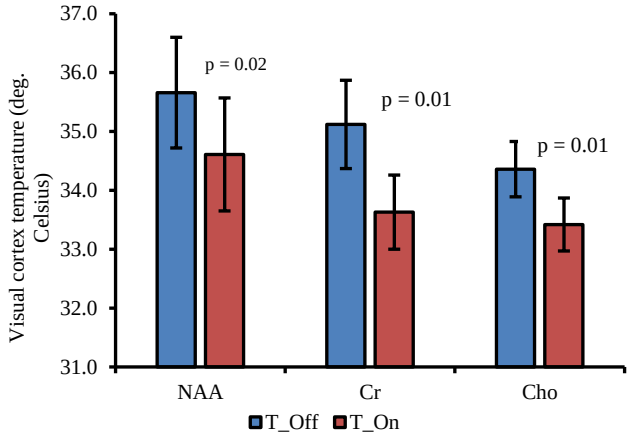

Figure 6. Visual cortex temperature change with the continuous activation paradigm

Discussion

This study measured brain temperature changes resulting from visual stimulation experiments. Without any further adjustments to the standard MR spectroscopy acquisition, the acquired data was processed to extract the frequency shift of the residual water peak relative to NAA, Cr, and Cho. The frequency difference was then substituted into previously deduced regression equations for each reference peak to estimate brain temperature for rest and stimulation acquisitions.

Consistent with a previous study [21], neuroactivation was associated with reduced brain temperature. However, the reduction in temperature was only significant with the continuous visual stimulation paradigm. Even though this might appear to contradict the expected result, it is possible that neuroactivation initially raises the physiological state and temperature above baseline limits, and when stimulation is sustained, the resulting increased cerebral blood flow and volume to the activation site rather carry away heat from the tissue. This could then adjust brain temperature to a lower level [1]. It has been observed that brain temperature rises again back to the baseline value shortly after neuroactivation, indicating brain warming post-neuronal activation [21].

Contrary to the finding of reduced visual cortex temperature in this study, a marginally elevated visual cortex temperature without an effect on metabolite concentrations has been observed elsewhere [22]. The possible reason for this observation is that an increase in heat production would be required to balance the cooling effects of the increased blood flow. The condition for this to occur is that the amount of heat increase should be at least equal to, or greater than, the amount of heat produced by the complete metabolism of the increased glucose utilization that accompanies neuroactivation.

According to Sukstanskii and Yablonskiy [12], brain temperature is influenced by an established equilibrium between the amount of heat produced by metabolism and carried away by blood under vessel diameter regulation. Temperature changes then occur if there is an unequal localized increase in blood flow relative to oxygen expenditure associated with neuroactivation. Within deep brain structures, temperature decreases with neuroactivation, which increases cerebral blood flow; temperature, however, increases in regions of reduced blood flow. Superficial brain regions, on the other hand, exhibit an exact reversal of this temperature effect, as they are cooler than incoming arterial blood, which exchanges heat with the environment [12].

This study demonstrates the feasibility of implementing MRS thermometry in fMRS to monitor brain temperature changes secondary to neuroactivation. The limitation of the use of previously deduced regression equations to convert the frequency offset to temperature values is that the voxel positions in the two studies are not necessarily similar. In addition, the accuracy of the regression fits, though about 90%, could have been better with many more data points ($n \geq 15$ healthy volunteers) rather than the seven volunteers ($n = 7$) used in the previous study [17]. Nonetheless, since the frequency offset varies linearly with the estimated brain temperature, the expected error will be systematic and linear in nature, affecting all measurements in the same way and magnitude. We acknowledge the lack of statistical power from our sample size ($n = 4$) to make generalizations on the average and range of temperature estimates measured. However, as a proof-of-concept study, the consistent observation of the frequency offset and proof of its utility in temperature estimation were met as the main study objectives.

It was unclear from the results what might have accounted for the only female volunteer in the study exhibiting a rather increased visual cortex temperature with the single activation paradigm when the general trend was a decrease. Unfortunately, the sample size was small, and there were not more females to determine if this trend was gender-specific or if it was a random finding. Future studies should use a larger sample size for both sexes in order to observe gender differences in the temperature response. Advancing age (over 60-65 years) is thought to be associated with lower body temperatures due to reduced body metabolism and other physiological processes [23]. The very narrow age range (29-31 years) of the volunteers in this study did not allow for an assessment of the effect of age on brain temperature. However, we did not observe a significant variation in brain temperature among them. Future studies should consider including a wide range of ages to carry out age-temperature association and inter-age group difference analysis on the results. In addition, postprocessing steps to denoise the fMRI data and reduce the effects of susceptibility artifacts in the activated maps were not conducted. This could have enhanced the accuracy of the identified activated volumes for fMRS voxel placement. At best, this study has established the possibility of monitoring brain temperature in fMRS studies and pointing to a general trend of reduced brain temperature with continuous visual stimulation.

Conclusion

By using a standard MRS acquisition sequence to implement MRS thermometry, occipital brain temperature response to single and continuous visual activation paradigms was studied in healthy volunteers. Temperature was estimated from the calibrated frequency shift of the water peak from the NAA, Cr and Cho peaks. Significant reduction in occipital brain temperature was observed with continuous, but not with single, activation paradigms. While this study could not establish age and sex effects on brain temperature response, it is important to mention that further study is warranted to explore the relationship between these variables and brain temperature response to visual stimulus.

Acknowledgments

We acknowledge the Scottish Imaging Network: A Platform for Scientific Excellence (SINAPSE) and the University of Glasgow, UK, for funding the PhD of the lead author, part of which resulted in the functional MRS data analyzed in this study.

The authors wish to thank the University of Ghana Medical Centre (UGMC) for providing access to their MRI system for the brain temperature calibration study, which resulted in the pre-determined regression equations. Special thanks go to Mr. George Nunoo, Head of Radiography, for his help with the data collection process.

References

1. Kiyatkin EA. Brain temperature and its role in physiology and pathophysiology: Lessons from 20 years of thermorecording. Temperature. 2019 Oct 2;6(4):271-333.
2. Mumuni AN, McLean J. Dynamic MR Spectroscopy of brain metabolism using a non-conventional spectral averaging scheme. Journal of neuroscience methods. 2017 Feb 1;277:113-21.
3. Mumuni AN, McLean J. Functional proton magnetic resonance spectroscopy of cerebral water and metabolites using eight radiofrequency excitations at 3.0 Tesla. EC proteomics and bioinformatics. 2017 Aug 29;1(1): 07-18.
4. Malonek D, Grinvald A. Interactions between electrical activity and cortical microcirculation revealed by imaging spectroscopy: implications for functional brain mapping. Science. 1996 Apr 26;272(5261):551-4.
5. Hennig J, Speck O, Deuschl G, Feifel E. Detection of brain activation using oxygenation sensitive functional spectroscopy. Magnetic resonance in medicine. 1994 Jan;31(1):85-90.
6. Zhu XH, Chen W. Observed BOLD effects on cerebral metabolite resonances in human visual cortex during visual stimulation: a functional 1H MRS study at 4 T. Magnetic resonance in medicine: An official journal of the international society for magnetic resonance in medicine. 2001 Nov;46(5):841-7.
7. Shih YY, Huang CJ, Büchert M, Chung HW, Liu YJ. INS-PRESS for functional MRS: simultaneous with-and without-water suppression spectral acquisition on visual cortex of human brains at 3T. In: Proceedings of the international society for magnetic resonance in medicine. 2009 (Vol. 17).
8. Ashworth ET, Cotter JD, Kilding AE. Impact of elevated core temperature on cognition in hot environments within a military context. European journal of applied physiology. 2021 Apr;121:1061-71.
9. Yin B, Fang W, Liu L, Guo Y, Ma X, Di Q. Effect of extreme high temperature on cognitive function at

different time scales: A national difference-in-differences analysis. Ecotoxicology and environmental safety. 2024 Apr 15;275:116238.
10. Hou K, Xu X. Ambient temperatures associated with reduced cognitive function in older adults in China. Scientific reports. 2023 Oct 13;13(1):17414.
11. Sun B, Wu J, Hu Z, Wang R, Gao F, Hu X. Human mood and cognitive function after different extreme cold exposure. International journal of industrial ergonomics. 2022 Sep 1;91:103336.
12. Sukstanskii AL, Yablonskiy DA. Theoretical model of temperature regulation in the brain during changes in functional activity. Proceedings of the national academy of sciences. 2006 Aug 8;103(32):12144-9.
13. Cady EB, D'Souza PC, Penrice J, Lorek A. The estimation of local brain temperature by in vivo 1H magnetic resonance spectroscopy. Magnetic resonance in medicine. 1995 Jun;33(6):862-7.
14. Vescovo E, Levick A, Childs C, Machin G, Zhao S, Williams SR. High-precision calibration of MRS thermometry using validated temperature standards: effects of ionic strength and protein content on the calibration. NMR in biomedicine. 2013 Feb;26(2):213-23.
15. Sharma AA, Nenert R, Mueller C, Maudsley AA, Younger JW, Szaflarski JP. Repeatability and reproducibility of in-vivo brain temperature measurements. Frontiers in human neuroscience. 2020 Dec 23;14:598435.
16. Childs C, Hiltunen Y, Vidyasagar R, Kauppinen RA. Determination of regional brain temperature using proton magnetic resonance spectroscopy to assess brain–body temperature differences in healthy human subjects. Magnetic resonance in medicine: An official journal of the international society for magnetic resonance in medicine. 2007 Jan;57(1):59-66.
17. Mumuni AN, Salifu MM, Abubakari MN. Brain temperature measurement by magnetic resonance spectroscopy thermometry using regression analysis. Medical physics. 2023 Dec 27; 11(2): 311-315.
18. Covaciu L, Rubertsson S, Ortiz-Nieto F, Ahlström H, Weis J. Human brain MR spectroscopy thermometry using metabolite aqueous-solution calibrations. Journal of magnetic resonance imaging: An official journal of the international society for magnetic resonance in medicine. 2010 Apr;31(4):807-14.
19. Verius M, Frank F, Gizewski E, Broessner G. Magnetic resonance spectroscopy thermometry at 3 tesla: importance of calibration measurements. Therapeutic hypothermia and temperature management. 2019 Jun 1;9(2):146-55.
20. Wang H, Wang B, Normoyle KP, Jackson K, Spitler K, Sharrock MF, Miller CM, Best C, Llano D, Du R. Brain temperature and its fundamental properties: a review for clinical neuroscientists. Frontiers in neuroscience. 2014 Oct 8;8:88894.
21. Rango M, Bonifati C, Bresolin N. Post-activation brain warming: a 1-H MRS thermometry study. PLoS one. 2015 May 26;10(5):e0127314.
22. Katz-Brull R, Alsop DC, Marquis RP, Lenkinski RE. Limits on activation-induced temperature and metabolic changes in the human primary visual cortex. Magnetic resonance in medicine: An official journal of the international society for magnetic resonance in medicine. 2006 Aug;56(2):348-55.
23. Blatteis CM. Age-dependent changes in temperature regulation–a mini review. Gerontology. 2012 Nov 11;58(4):289-95.